*Supporting Information for:*

# Dynamic sampling from *ex vivo* adipose tissue using droplet-based microfluidics supports separate mechanisms for glycerol and fatty acid secretion

Md Moniruzzaman,[a] Andresa B. Bezerra,[a] Md Mohibullah,[a] Robert L. Judd,[b] James G. Granneman,[c] and Christopher J. Easley*,[a]

a. Department of Chemistry and Biochemistry, Auburn, AL, USA

b. Department of Anatomy, Physiology, and Pharmacology, Auburn, AL, USA

c. Center for Molecular Medicine and Genetics, Wayne State University School of Medicine, Detroit, MI, USA.

Correspondence: chris.easley@auburn.edu

**Supporting Information (SI) Contents:**

## SUPPLEMENTARY METHODS

### Microfluidic Master Wafer Fabrication

This study utilized standard multilayer soft lithography methods to fabricate three-layer microfluidic devices. To create the fluidic channel, merging channel, incubation channel and pneumatic valve control channels, two master wafers were first made using soft lithography. The channel designs (Figure S-1) were created using Adobe Illustrator and printed by Fineline Imaging (Colorado Spring, CO) at 50,800 dpi resolution to serve as the photolithographic masks. For the pneumatic control channel (thin lower layer), a silicon wafer was spin-coated with a ~25-µm thickness negative photoresist (SU-8 2015) layer and soft baked at 65 °C for 1 min, 95 °C for 5 min, and 65 °C for 1 min, then it was allowed to cool to room temperature (RT). UV exposure through the pneumatic channel mask was done for 120 s on an in-house built UV LED exposure unit (designed from Erickstad, et al.), followed by hard baking for 65 °C for 1 min, 95 °C for 5 min, and 65 °C for 1 min; the system was then cooled passively to RT. The exposed photoresist was then treated with SU-8 developer solution for ~5 min with rocking, washed with isopropanol (IPA), then dried with a stream of $N_2$ gas. For the fluidic merging and incubation channels (thickest layer of flow channels), a silicon wafer was spin-coated with ~55-µm thick negative photoresist (SU-8 2050) and soft baked at 65 °C for 3 min, 95 °C for 7 min, and 65 °C for 1 min, then allowed to cool to RT. UV exposure through the fluidic merging/incubation channel mask was done for 90 s. Hard baking was then done 65 °C for 2 min, 95 °C for 6 min, and 65 °C for 1 min; the system was then cooled to RT. Treatment with SU-8 developer solution was done for ~7 min, followed by washing IPA and drying with a stream of $N_2$ gas. For the valve-actuated fluidic channel layer, a ~35-µm thick layer of positive photoresist (AZ 40 XT) was spun onto the same silicon wafer which already included merging and incubation channel templates. The AZ photoresist was soft baked at 65 °C for 5 min, 95 °C for 5 min, 115 °C for 5 min, and 65 °C for 1 min, followed by passive cooling to RT. UV exposure through the third mask was done for 90 s. The hard bake was done at 65 °C for 1.5 min, 95 °C for 1.5 min, 105 °C for 1.5 min, and 65 °C for 1 min, followed by cooling to RT. The wafer was then treated with AZ developer solution for 5 min, followed by a water wash then drying step using a stream of $N_2$ gas. To reflow and round out the cross-section of the AZ-defined fluidic channel templates, we heated the wafer for 65 °C for 1 min, 95 °C for 1 min, 120 °C for 10 min, then cooling down to 60 °C by placing it in an oven for at least 30 min. The two master wafers were later used for PDMS molding.

### Microdevice Fabrication

The upper layer of the microfluidic device was fabricated by pouring ~36 g of a mixed PDMS precursor mixture (with a 5:1 ratio of monomer to curing agent) onto the flow channel wafer. Meanwhile, 7.5 g of PDMS precursor (with a 20:1 ratio of monomer to curing agent) were spin-coated onto a separate silicon wafer, which served as the lower pneumatic membrane, at 2100 rpm for 45 s. Both layers were baked in an oven at 60 °C for approximately 30 minutes.

Next, the thick fluidic layer was peeled off, cut, punched, and washed before being aligned to the valve channel. The assembled layers were then baked overnight in the oven at 60 °C. To irreversibly bind the PDMS to a thin cover glass, plasma oxidization was used after the PDMS was peeled from the wafer, diced, and punched. After plasma oxidation, devices were baked overnight in the oven at 60 °C. Finally, the microfluidic device was assembled and ready to use, and it was stored at room temperature.

If PDMS adhesion became problematic, prior to use for molding, the silicon wafers were exposed to trimethylsilyl chloride vapor for 30 min to enhance PDMS removal. The channels were later characterized by imaging the channel cross section after slicing an assembled PDMS device.

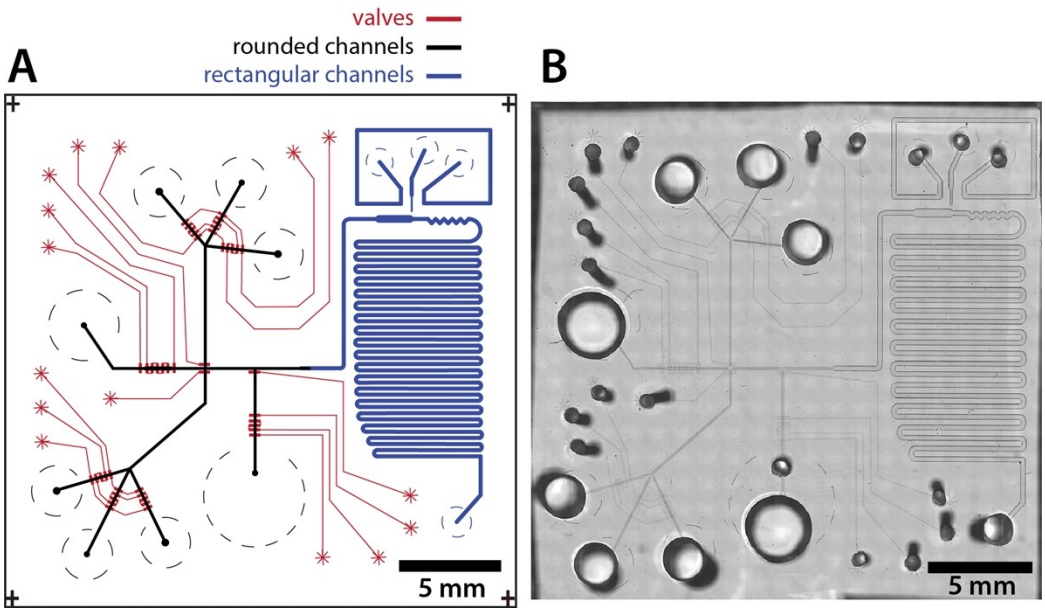


**Figure S-1.** Microfluidic device design. (A) An overlay of the three photomasks used for photolithographic patterning of the device master onto a silicon wafer. (B) High resolution microscope image of a completed device.

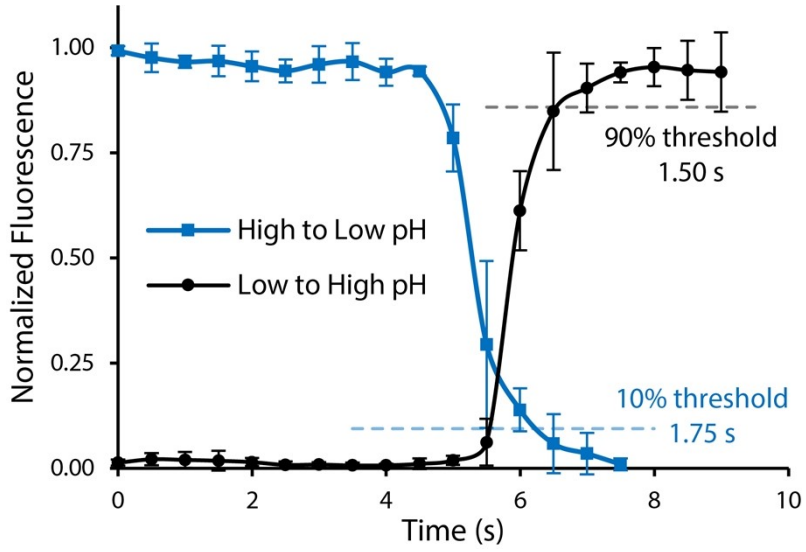


**Figure S-2.** Tissue stimulation resolution within the 3D-printed trap was determined by imaging pH-responsive glass beads and switching pH in the stimulant reservoir during valve-based pumping. These data show that stimulation resolution is less than 2 s.

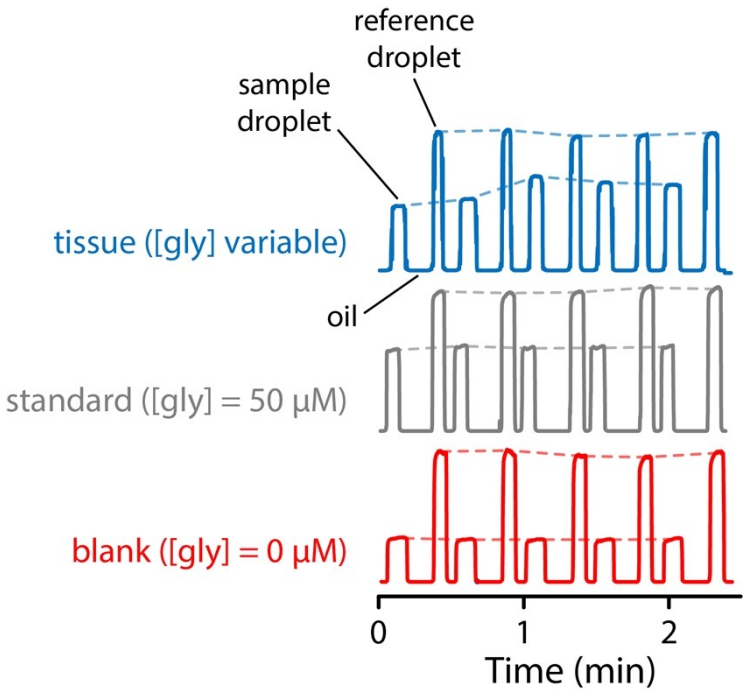


**Figure S-3.** Example raw data sets from the blank (0 µM glycerol; red trace), a calibration standard (50 µM glycerol; gray trace), and a tissue experiment where glycerol is varying. The y-axis data represent the 14-bit camera intensity, and scalings on all data are equivalent, while data are offset for clarity. Dashed lines for each trace are shown as a guide to the reader's eye, showing an estimated magnitude for each droplet; these lines show that calibration standard and continuous reference signals were constant while tissue signals were variable.

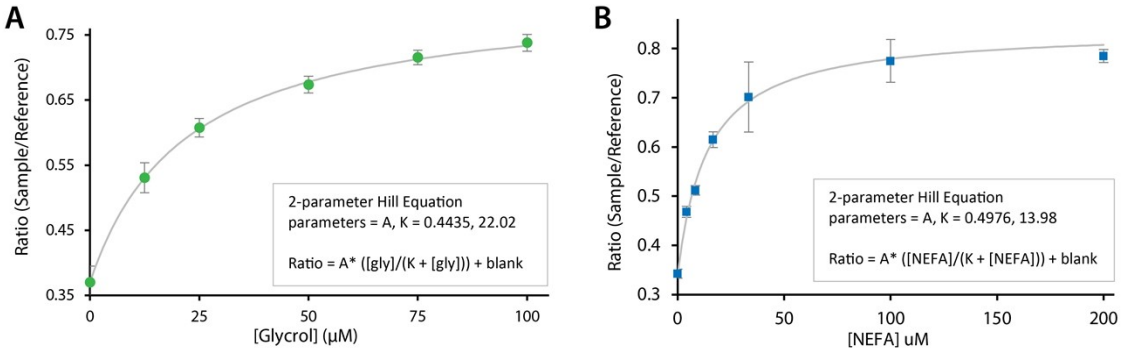


**Figure S-4.** Calibration curves for coupled enzyme assays obtained on-chip by imaging at the region of interest (ROI) in the incubation and readout channel. (A) Glycerol was calibrated in the range from 0 to 100 µM, while (B) NEFA was calibrated in the range from 0 to 200 µM. The 3 LOD for glycerol was 6 µM (70 fmol), while the LOD for NEFA was 0.9 µM (10 fmol). The 2-parameter, sigmoidal Hill curves were determined with nonlinear least squares fitting to these data, and the inverse equation was used to determine the concentration within each detected droplet based on the measured sample/reference ratio.

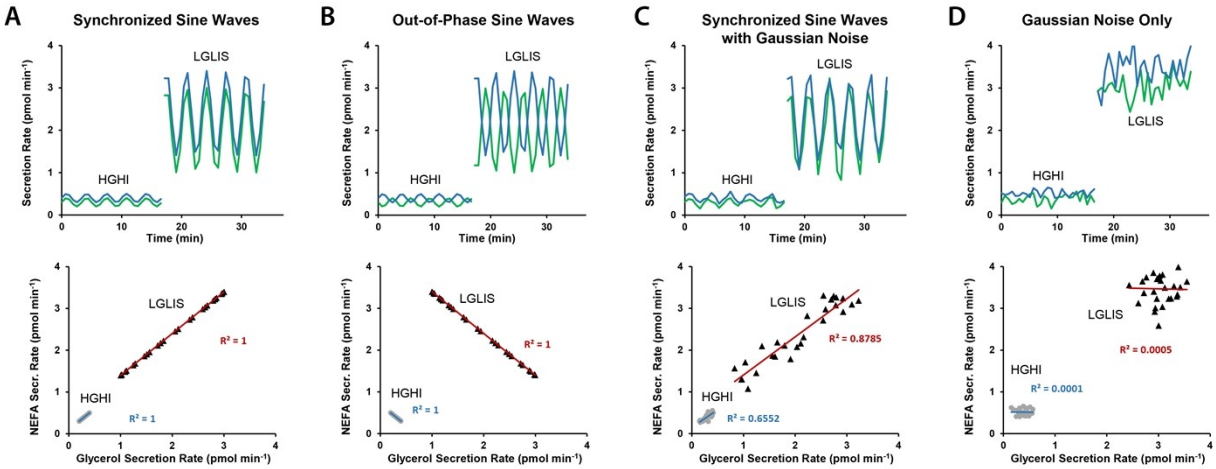


**Figure S-5.** Simulations of oscillatory glycerol and NEFA secretion (top) to illustrate the effects on linear regression plots (bottom) between data sets. The data was simulated with the same temporal resolution and general secretion rate ranges measured in the experiments, and traces were slightly offset vertically for clarity. (A) Synchronized sine waves at both HGHI and LGLIS conditions result in $R^2$ values of 1.0 and a positive slope. (B) When sine waves are out of phase by 180°, the linear regression plots still result in $R^2$ = 1.0, but with negative slope. (C) Synchronized sine waves with Gaussian noise (20-30% of the signal magnitudes) added still show strong correlations but with lower $R^2$ values, while (D) simulations with only Gaussian noise result in essentially zero correlation.

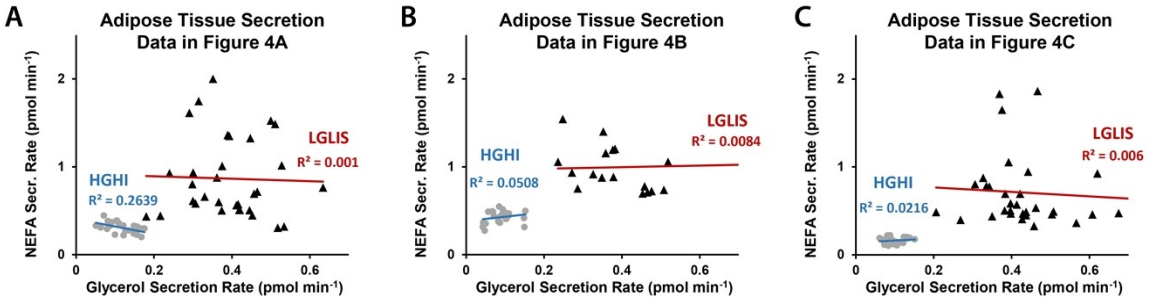


**Figure S-6.** Linear regressions from secretion data measured by the µADC. Regression plots are shown for data from (A) Figure 4A, (B) Figure 4B, and (C) Figure 4C from the main text. In either the HGHI regression plots (blue) or LGLIS regression plots (red), NEFA secretion rate data is plotted against glycerol secretion rate data from the same explant. Observed correlations were very weak to negligible, suggesting different mechanisms of release for glycerol and NEFA.